Carbohydrate Polymers 86 (2011) 852–859

Contents lists available at ScienceDirect

Carbohydrate Polymers

journal homepage: www.elsevier.com/locate/carbpol

Wheat bran arabinoxylans: Chemical structure and film properties of three isolated fractions

Ying Zhang[a,b], Leena Pitkänen[c], Jacques Douglade[d], Maija Tenkanen[c], Caroline Remond[a,b,*], Catherine Joly[e]

[a] INRA, UMR614, Fractionnement des AgroRessources et Environnement, F-51686 Reims, France
[b] Université de Reims Champagne Ardenne, UMR614, Fractionnement des AgroRessources et Environnement, F-51686 Reims, France
[c] Department of Food and Environmental Sciences, University of Helsinki, P.O. Box 27, 00014 Helsinki, Finland
[d] Faculté des Sciences, Laboratoire d'Electrochimie et Chimie du Solide, Reims cedex, France
[e] Biodymia EA3733, Université de Lyon, Université Lyon1, IUT GB, Technopole Alimentec, Bourg en Bresse, France

ARTICLE INFO

Article history:
Received 6 April 2011
Received in revised form 10 May 2011
Accepted 18 May 2011
Available online 26 May 2011

Keywords:
Wheat bran
Arabinoxylans
Substitutions
Films
Material properties

ABSTRACT

The purpose of this study was to isolate arabinoxylans (AX) from wheat bran in order to further investigate the impact of their composition and structure on several physico-chemical properties used for food packaging films. Three hemicellulose fractions were alkali-extracted from destarched wheat bran and fractionated according to their solubility. Moreover, AX were further purified by elimination of β-glucans. The three AX fractions displayed a wide range of Ara/Xyl ratios varying from 0.2 to 1.3, contained various patterns of arabinose substitutions and different molar mass (152 000–218 000 Da). The crystalline morphology, the beta transitions and water sorption properties of AX-based films were well correlated with the Ara/Xyl ratios of xylans. When arabinose content decreased, the films were more crystalline and the beta transitions decreased as well as the water uptake at high relative humidity. The local chain motion decreased in the amorphous parts for highly substituted xylans. Furthermore, the presence of co-extracted β-glucans modified the properties of the AX-films.

1. Introduction

New biodegradable materials from renewable biomass represent alternative material sources, notably for food packaging as self standing films or coating. In such applications, materials with good gas barrier properties are required. Both starch and proteins have been reported to demonstrate interesting oxygen barrier properties (Dole, Joly, Espuche, Alric, & Gontard, 2004; Hong & Krochta, 2006). Hemicelluloses (HC) such as xylans are also good candidates for food packaging applications. Xylans are considered to be the second most abundant polysaccharide in the plant kingdom after cellulose. When isolated, these heteropolysaccharides form a dense macromolecular network with low mobility, which leads to excellent oxygen barrier properties (Grondahl, Eriksson, & Gatenholm, 2004). All polar polymers, xylan and particularly arabinoxylan (AX) based films possess good intrinsic barrier properties against apolar migrants (i.e. oxygen or aromas) (Grondahl et al., 2004; Hartman, Albertsson, Lindblad, & Sjoberg, 2006; Hansen & Plackett, 2008). Moreover, new properties can be achieved or investigated thanks to the high intrinsic natural variability of AX in plant cell walls (Ebringerová, 2005; Pastell, Virkki, Harju, Tuomainen, & Tenkanen, 2009). For example, the Ara/Xyl ratio can be either tailored through enzymatic modification (Höije, Sternemalm, Heikkinen, Tenkanen, & Gatenholm, 2008) or simply obtained from a controlled isolation process as illustrated in this study.

Wheat bran is an abundant industrial by-product generated during the milling operation, and represents an interesting biomass for further applications. Major constituents in wheat bran are non-starch polysaccharides (46%), starch (10–20%), proteins (15–22%) and lignin (4–8%) (Bergmans, Beldman, Gruppen, & Voragen, 1996). AX, which are classified as hemicelluloses, are the major non-starch polysaccharides in wheat bran (Bataillon, Mathaly, Nunes Cardinali, & Duchiron, 1998). AX consist of α-(1 → 4)-linked D-xylopyranosyl residues decorated with α-(1 → 2)- and/or α-(1 → 3)-linked L-arabinofuranosyl units. To a lesser extent, some xylopyranosyl residues are also substituted with a 4-*O*-methyl ether glucuronic acid (Brillouet, Joseleau, Utille, & Lelievre, 1982). Furthermore, acetyl groups as well as hydroxycinnamoyl groups have been reported to be present in AX from graminaceaous plants (Nishimura, Ishihara, Ishii, & Kato, 1998; Ring & Selvendran, 1980). β-Glucans, unbranched polysaccharides composed of

* Corresponding author at: INRA, UMR614, Fractionnement des AgroRessources et Environnement, F-51686 Reims, France. Tel.: +33 3 26 35 53 64; fax: +33 3 26 35 53 69.
E-mail address: caroline.remond@univ-reims.fr (C. Remond).

0144-8617/$ – see front matter © 2011 Elsevier Ltd. All rights reserved.
doi:10.1016/j.carbpol.2011.05.036

D-glucopyranosyl (1 → 4) and (1 → 3)-linked residues, are also part of non-starch polysaccharides (Henry, Martin, & Blakeney, 1987).

AX are generally extracted either by hot water and/or aqueous alkali and can be fractionated according to their solubility in different solvents such as ethanol (Ebringerova & Heinze, 2000). The yield as well as the composition of the extracted polysaccharides largely depends on the isolation method used. During AX isolation, other plant cell wall components such as β-glucans, proteins or phenolic molecules can be recovered (Izydorczyk & Biliaderis, 2000; Höije, Gröndahl, Tømmeraas, & Gatenholm, 2005).

The aim of this study was to investigate the properties of AX and their potential for use as packaging films or coatings. As already discussed, AX are interesting macromolecule resources because their physico-chemical properties can be modified due to their intrinsic natural variability. To investigate such promising potential, our study covers the extraction process of AX (laboratory scale), film formation by water casting and film characterization. In this context, the strategy developed was (i) to isolate various populations (fractions) of AX from destarched wheat bran by performing an alkali extraction followed by controlled precipitation steps in water or ethanol, (ii) to investigate their chemical composition and structural characteristics (substitution patterns, molecular weights), (iii) to make films for each AX population by casting, and finally (iv) to investigate film physico-chemical properties (X-ray measurements, water sorption, macromolecular mobility depending on the fraction characteristics).

2. Materials and methods

2.1. Materials

Hemicelluloses (HC) were alkali-extracted from destarched wheat bran provided by ARD (Pomacle, France). Extraction (Fig. 1) was performed according to an adapted method of Zinbo and Timell (1965).

Ground destarched wheat bran (60 g) was suspended in 1 L of 24% KOH (w/v in water) containing 1% $NaBH_4$ (w/v). Extraction occurred at room temperature with stirring for 3 h. HC were recovered by filtration after pH neutralization with 0.6 volumes of glacial acetic acid and precipitation with 6 volumes of ethanol during one night at 4 °C. Precipitated HC were collected after washing with distilled water at room temperature and filtration through a sintered glass filter (porosity 2). In order to fractionate HC according to their solubility in water, the obtained precipitates were solubilized in hot water (60 °C) with stirring for 10 min. The water soluble hemicelluloses were separated from water insoluble ones (WI-HC) by centrifugation, and this process was repeated six times. Water soluble HC were further fractionated by ethanol with a final concentration of 50% (v/v). After one night at 4 °C, water and ethanol soluble HC (WS–ES-HC) and water soluble/ethanol insoluble HC (WS–EI-HC) were separated by centrifugation (6000 rpm during 20 min). HC were dialyzed with deionized water (MWCO 3500) and freeze-dried.

Aliquots of WI-HC and WS–EI-HC were further purified in order to eliminate β-glucans. Enzymatic hydrolysis was performed with 0.1 IU lichenase/g hemicellulose (lot 70801, 330 IU/mg, Megazyme) and 6.5 CBU β-glucosidase/g hemicellulose (NS-50010, lot DCN00211, 250 CBU/g, Novozymes). Hydrolysis was carried out in 50 mM Tris–HCl pH 6.8 for 24 h at 60 °C after which the samples were dialyzed with deionized water for 48 h (MWCO 3500) and freeze-dried. Samples treated with lichenase correspond to arabinoxylans (AX) and were named: WI-AX and WS–EI-AX. The fraction obtained after dialysis without lichenase treatment was named WS–ES-AX (Fig. 1).

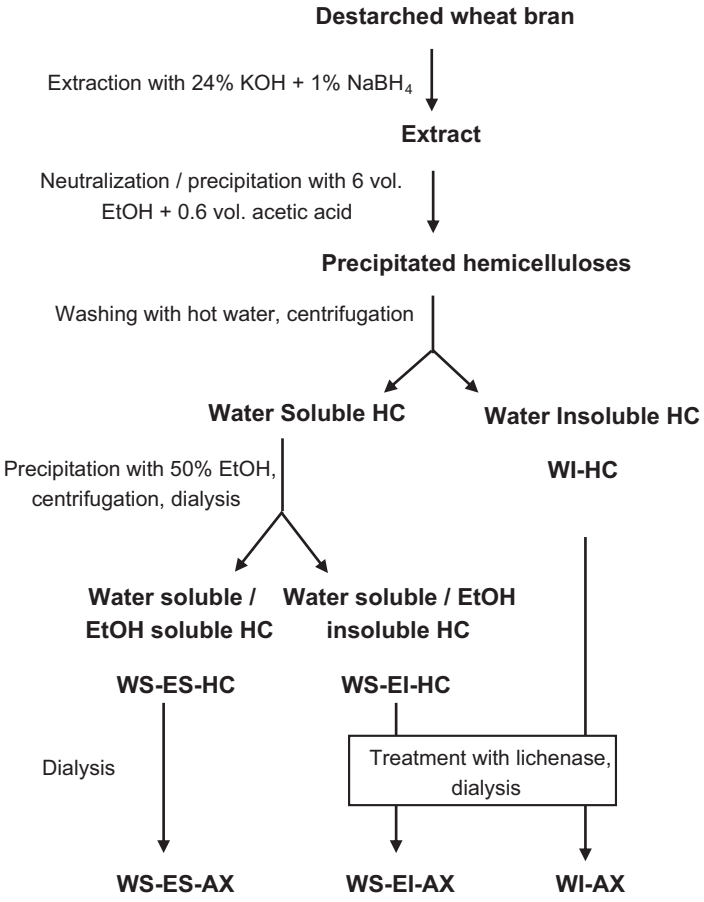

Fig. 1. Multi-step preparation of hemicellulose fractions from destarched wheat bran. HC, before lichenase treatment and arabinoxylan AX, after lichenase treatment.

2.2. Analysis of the isolated HC and AX

The neutral monosaccharide composition was determined in triplicate by a high-performance anion exchange chromatography with pulse amperometric detection (HPAEC-PAD) using fucose as an internal standard as previously described (Benamrouche, Crônier, Debeire, & Chabbert, 2002). AX were hydrolyzed in 1.5 M sulphuric acid for 2 h at 100 °C with stirring. After hydrolysis, the samples were diluted 2-fold, filtered and injected into a CarboPac PA 1 anion-exchange column (4 × 250 mm, Dionex). Protein content was determined from total N content using an elemental analyser (NA 1500, Carlo Erba) coupled to a mass spectrometer (Fisons Isochrom). Total N content was converted into protein content with the equation: $N \times 5.7$ (Beaugrand, Crônier, Debeire, & Chabbert, 2004). Klason lignin was quantified as the acid-insoluble residue remaining after sulphuric acid hydrolysis (Monties, 1984). Samples (300 mg) were suspended in 3 mL of 72% (w/w) H_2SO_4 for 2 h at 20 °C then hydrolyzed at 100 °C with 1 M sulphuric acid. The remaining residues were dried at 105 °C and weighed, then ignited for 3 h at 550 °C. The lignin content was determined by subtracting the weighed ash.

2.3. Enzymatic hydrolysis and HPAEC-PAD fingerprinting of AX

The AX samples (5 g/L) in 0.02 M sodium acetate buffer, pH 5.0, were hydrolyzed to oligosaccharides with Shearzyme 500L (CD00220, endo-(1-4)-D-xylanase, 49 100 nkat/mL, Novozymes, Bagsvaerd, Denmark) using an enzyme ratio of 10 000 nkat/g xylan, at 40 °C for 48 h, then the samples were heated to 100 °C for 10 min to stop the reaction. The hydrol-

ysis products were analyzed using HPAEC-PAD as described previously by Pastell et al. (2009). Peaks were identified according to their retention times compared to those of purified, structurally-defined arabinoxylo-oligosaccharides: A^3X (α-L-Araf-(1 → 3)-β-D-Xylp-(1 → 4)-D-Xyl), $A^{2+3}X$ (α-L-Araf-(1 → 2)-[α-L-Araf-(1 → 3)]-β-D-Xylp-(1 → 4)-D-Xylp) and $A^{2+3}XX$ (α-L-Araf-(1 → 2)-[α-L-Araf-(1 → 3)]-β-D-Xylp-(1 → 4)-β-D-Xylp-(1 → 4)-D-Xylp) (abbreviations according to Pastell, Tuomainen, Virkki, & Tenkanen, 2008). Peak identification was also verified by treating the Shearzyme hydrolysates with α-arabinofuranosidase. After addition of α-arabinofuranosidase (5000 nkat/g xylans) to the AX hydrolysates (500 μL), samples were mixed and incubated for 24 h at 40 °C to release arabinose side groups.

2.4. HPSEC analysis

HPSEC analysis of AX was performed using a 0.01 M solution of LiBr in DMSO as an eluent. The samples (c = 4 mg/mL) were dissolved in the eluent at room temperature for 4 days to ensure solubility and filtered before analysis with 0.45 μm syringe filters (GHP Acrodisc 13, Pall Corp., Ann Arbor, MI, USA). The HPSEC equipment consisted of an integrated autosampler and pump module (GPC max, Viscotek Corp., Houston, TX, USA), two linear type columns (Shodex LF-804, 8 × 300 mm, Showa Denko, Tokyo, Japan), a guard column (Shodex LF-G, 4.6 × 10 mm), a UV-detector (Waters 486 Tunable Absorbance Detector, Milford, MA, USA), a combined light scattering and viscometric detector (270 Dual Detector, Viscotek Corp.) and a refractive index (RI) detector (VE 3580, Viscotek Corp.). The light scattering detector (λ_0 = 670 nm) included two scattering angles: 7° (low angle light scattering, LALS) and 90° (right angle light scattering, RALS). The Viscotek Dual Detector was calibrated with the pullulan standard (M_w = 47 300, Polymer Laboratories, Shropshire, UK). The flow rate was 1 mL/min and the columns were thermoregulated in a column oven (Croco-cil 100-040-220P, Cluzeau Info Labo, Sainte-Foy-la-Grande, France) at 40 °C. The molar mass averages were calculated based on the light scattering/viscometry method (Fishman, Doner, Chau, & Hoagland, 2000) using the dn/dc value of 0.064 mL/g (Goring & Timell, 1960). The UV detector at λ_0 = 280 nm was used for monitoring protein and lignin impurities. Differences in chain flexibilities between the AX samples were investigated by comparing the persistence length values (L_p) calculated from the intrinsic viscosity and the molar mass data obtained from HPSEC using the Bohdanecký model (Bohdanecky, 1983; Pitkanen, Virkki, Tenkanen, & Tuomainen, 2009).

2.5. Film preparation

HC or AX fractions (400 mg in 20 mL deionized water) were mixing by stirring at 95 °C for 60 min. The solutions were casted on polystyrene Petri dishes (diameter = 29 mm) and dried at room temperature with 50% relative humidity (RH). The films obtained were transparent, with a 35 μm average thickness. The films were stored under constant RH (54 and 85% RH) for one week before performing various measurements (see below). The humidity was controlled by aqueous solutions of $Mg(NO_3)_2$ (54% RH) and KCl (85% RH) (Vertucci & Roos, 1993) respectively at 20 °C.

2.6. X-ray analysis

The AX films were characterized using X-ray diffraction. Wide angle X-ray scattering measurements were carried out with a D8 ADVANCE BRUKER using Cu Kα radiation (wave length = 1.54 Å). The 2θ was varied from 15° to 35° at a rate of 1°/min and a step of 0.1°.

2.7. Water sorption isotherms

Film samples (2–5 mg) were suspended from the beam of a microbalance (IGA, Intelligent Gravimetric Analyzer, IGA-Hiden Ltd.) at 20 °C, with humidity varying from 10% to 90%. The sample water uptake was recorded at equilibrium for the chosen RHs (10–90% at 10% intervals). The dry mass was obtained after the application of a drying sequence (120 min at 40 °C, then 480 min at 20 °C).

The water uptake was calculated by:

$$\text{Water uptake } (\%) = 100\frac{m_{\text{moist}} - m_{\text{dry}}}{m_{\text{dry}}}$$

2.8. Dynamic electrical analysis

For dielectric testing, a TA Instruments DiElectrical Analyzer (DEA) was used in a multi-frequency mode. The pre-hydrated films with AX and HC were positioned between 2 electrodes (sputter coated model of TA instruments). A constant force of 340 N was applied to the film during the heating ramp (3 °C/min) under Nitrogen flow. A modification of the sample holder was necessary in order to prevent water evaporation during measurement. A gas barrier rubber O ring was added. This seal was specially designed and cured from crude formulation provided by Viton®. The water content of the equilibrated sample did not vary up to 150 °C for samples that did not exceed 20 wt% water content. The transition temperature was taken at the maximum tan δ peaks.

3. Results and discussion

3.1. Isolation, fractionation and composition of HC and AX

The yields of HC and AX fractions are presented in Table 1 according to the extraction process illustrated in Fig. 1. Three fractions were obtained by alkali-extraction of 60 g of destarched wheat bran and subsequent fractionation according to their solubility in water and in 50% ethanol. They were coded WI-HC (water insoluble), WS–EI-HC (water soluble–ethanol insoluble) and WS–ES-AX (water soluble–ethanol soluble) thus giving a total of 10.2 g of hemicelluloses isolated from the total wheat bran. Knowing that AX accounts for 40% of dry matter in the destarched wheat bran used in this study (Beaugrand et al., 2004), 42.5% of the AX originally present were extracted by this process. Xylan extraction yields are greatly affected by the plant species as well as the type of plant material, but also by the strength and nature of the alkali, as well as the extraction time and temperature. Brillouet et al. (1982) obtained a xylan recovery of 13% with a sodium hydroxide-based extraction procedure from wheat bran.

The purity of HC and AX fractions was relatively high as carbohydrate content was between 72 and 87% of dry matter for all fractions (Table 1). The alkali-isolation of xylans from seed endosperm and seed coats (bran) is generally described to be complicated as some others components (e.g. proteins, starch, glucans, phenolics) are also extracted during the isolation procedure (Ebringerova & Heinze, 2000; Höije et al., 2005).

Hemicellulose isolated from wheat bran mainly consists of arabinoxylans as demonstrated by the high content of xylose and arabinose in the WI-HC, WS–EI-HC and WS–ES-AX fractions which contained respectively 64%, 63% and 68% of (Xyl + Ara). As the wheat bran used for this study was destarched, glucose, mainly present in WI-HC and WS–EI-HC, could be present as β-glucans. A lichenase and β-glucosidase treatment was thus performed in order to purify the HC fractions. The glucose content was reduced in both these fractions from 13% to 2% for the WI fraction and from 18% to 6% in the WS-EI one. WS–ES-AX had a very low amount of glucose

Table 1
Quantity, yield and composition of HC and AX fractions.

	WI-HC	WS–EI-HC	WI-AX	WS–EI-AX	WS–ES-AX
Quantity (g)	6.8	2.2	7.2	2.0	1.2
Yield (%)[a]	11.3	3.7	12.0	3.3	2.0
% Neutral sugars[b,c]	78	84	83	87	72
% Ara[b]	12	29	14	35	39
% Xyl[b]	52	34	66	44	29
% Glc[b]	13	18	2	6	2
% Gal[b]	1	3	1	2	2
Ara/Xyl[d]	0.2	0.9	0.2	0.8	1.3
Glc/Xyl[d]	0.2	0.4	0.03	0.08	0.08
% Protein[b]	1.4	1.3	10.8	11.8	5.6
% Klason lignin[b]	0.8	1.2	–	–	2.0

[a] % from wheat bran.
[b] % related to dry matter.
[c] % corresponding to the sum of Ara + Xyl + Glc + Gal.
[d] % expressed in mole ratios.

(1.3%), as a result this fraction was not treated by lichenase. Sugar analysis indicated that the amount of uronic acids was very low in all AX fractions (data not shown). Substitution along the main chains is one factor reported to improve the solubility of xylans in water (Andrewartha, Phillips, & Stone, 1979). The different steps of our extraction procedure, based on solubility properties in water and in ethanol–water (50/50), led to the isolation of three HC fractions and further AX populations with increasing Ara/Xyl ratio from WI-AX (A/X = 0.2), to WS–EI-AX (0.8) to WS–ES-AX (1.3).

The protein content of AX fractions from wheat bran is presented in Table 1. The protein content was rather low before the lichenase and β-glucosidase treatment (from about 2 to 5%). Destarched wheat bran has been reported to contain between 10 and 18% protein depending on the wheat species (Beaugrand et al., 2004). In our study, the protein content increased almost ten-fold (around 10–12%) after treating the WI-AX and WS–EI-AX fractions by lichenase and β-glucosidase. This indicating that the enzyme treatments led to concomitant sample contamination with proteins, and consequently to a slightly higher yield for the WI-fraction (Table 1).

The Klason lignin content was determined for the three HC fractions before lichenase treatment (Table 1). Lignin content was shown to be less than 2% for all three HC fractions. It is important to note that the destarched wheat bran used in our study was poorly lignified as the lignin content had been estimated to be less than 5% of dry matter in a previous study (data not shown).

3.2. Analysis of the substitution patterns of AX

The AX fractions were hydrolyzed with an endoxylanase (Shearzyme, glycoside hydrolase family 10 enzyme) and the obtained oligosaccharide profiles were analyzed for further information on the structural differences between the isolated AX fractions. The identification of arabinoxylo-oligosaccharides (AXOS) after Shearzyme hydrolysis of wheat arabinoxylans was recently reported by Pastell et al. (2009). All three AX fractions resulted in similar AXOS profiles but with varying proportions (Fig. 2). The main oligosaccharide peak in all hydrolyzates was xylobiose (X_2). The next peak in the HPAEC-PAD chromatograms at 30.7 min was identified as A^3X. This confirmed that the main substituent in WI-AX is a (1 → 3) linked α-L-Araf. The amount (peak height) of A^3X was clearly lower in the WS–EI-AX and WS–ES-AX hydrolyzates, respectively. The amount of di-substituted β-D-Xylp $A^{2+3}X$ (retention time 32.6 min) and $A^{2+3}XX$ (retention time 33.8 min) increased respectively from the water insoluble WI-AX to the water-soluble WS–EI-AX and WS–ES-AX, indicating an increased amount of di-substituted β-D-Xylp in the water-soluble AX fractions. The different AXOS peaks were not quantified in this study. According to Pastell (2010), the response factors of $A^{2+3}X$ and $A^{2+3}XX$ are 70% and 50% of that of A^3X respectively. It could thus be estimated that the amount of mono- and di-substituted AXOS in the WS–EI-AX hydrolysate was about equal.

Moreover, the degree of hydrolysis of the AX fractions clearly decreased with increasing Ara/Xyl ratio as seen by the decrease of the xylobiose (X^2) peak in the chromatograms. Even though Shearzyme is not able to hydrolyze the most densely substituted AX, the AXOS profile was previously found to closely reflect the structural differences in AX as analyzed by NMR spectroscopy (Pastell et al., 2009).

3.3. HPSEC analysis of AX

The HPSEC analysis of the purified AX fractions was performed in DMSO which was recently shown to be better solvent (and eluent) for cereal AX than an aqueous salt solution (Pitkanen et al., 2009). As indicated by the RI and viscosity signals (Fig. 3), the three AX fractions eluted at the same position. The overlay chromatogram of the viscosity signals, however, revealed the differences in intrinsic viscosities seen as varying signal intensities (Fig. 3B). The determined average values for intrinsic viscosity supports this conclusion (Table 2). The $[\eta]$ for WI-AX was the highest whereas the WS–ES-AX fraction presented the lowest $[\eta]$. Generally, the intrinsic viscosity of linear polymers increases with increasing molar mass but in this case the molar mass for WS–ES-AX with the lowest $[\eta]$ is higher in comparison with WI-AX and WS–EI-AX (Table 2). Thus, the molecular density of the WS–ES-AX sample seems to be higher in respect to the other two samples.

Slight UV signals were detected in all samples, but the peak apexes existed at higher elution volumes than the viscosity peaks containing the majority of the polymeric material (Fig. 3C). Although the signal intensities were low, the amount of UV absorbing material was clearly different in each fraction. The UV signal was the highest for WS–ES-AX, and could originate from lignin which is soluble in DMSO. The Klason lignin content was slightly higher for WS–ES-AX than for WI-AX and WS–EI-AX (Table 1).

The average molecular weights of eluted samples varied from 152 000 to 218 000 g/mol for the studied fractions. According to viscosity detection, the WS–ES-AX sample was more compact than the WI-AX and WS–EI-AX ones, and the possibility of aggregation cannot be excluded. The phenolic compounds might cross-link the shorter AX chains to form assemblies (WS–ES-AX showed the strongest UV signal, Fig. 3C). As indicated by the monosaccharide composition analysis, the Ara/Xyl ratio of WS–ES-AX was as high as 1.3 but this high arabinose content cannot, in itself, explain the low intrinsic viscosity value or the possible aggregation. In fact, a slight increase in intrinsic viscosity values have

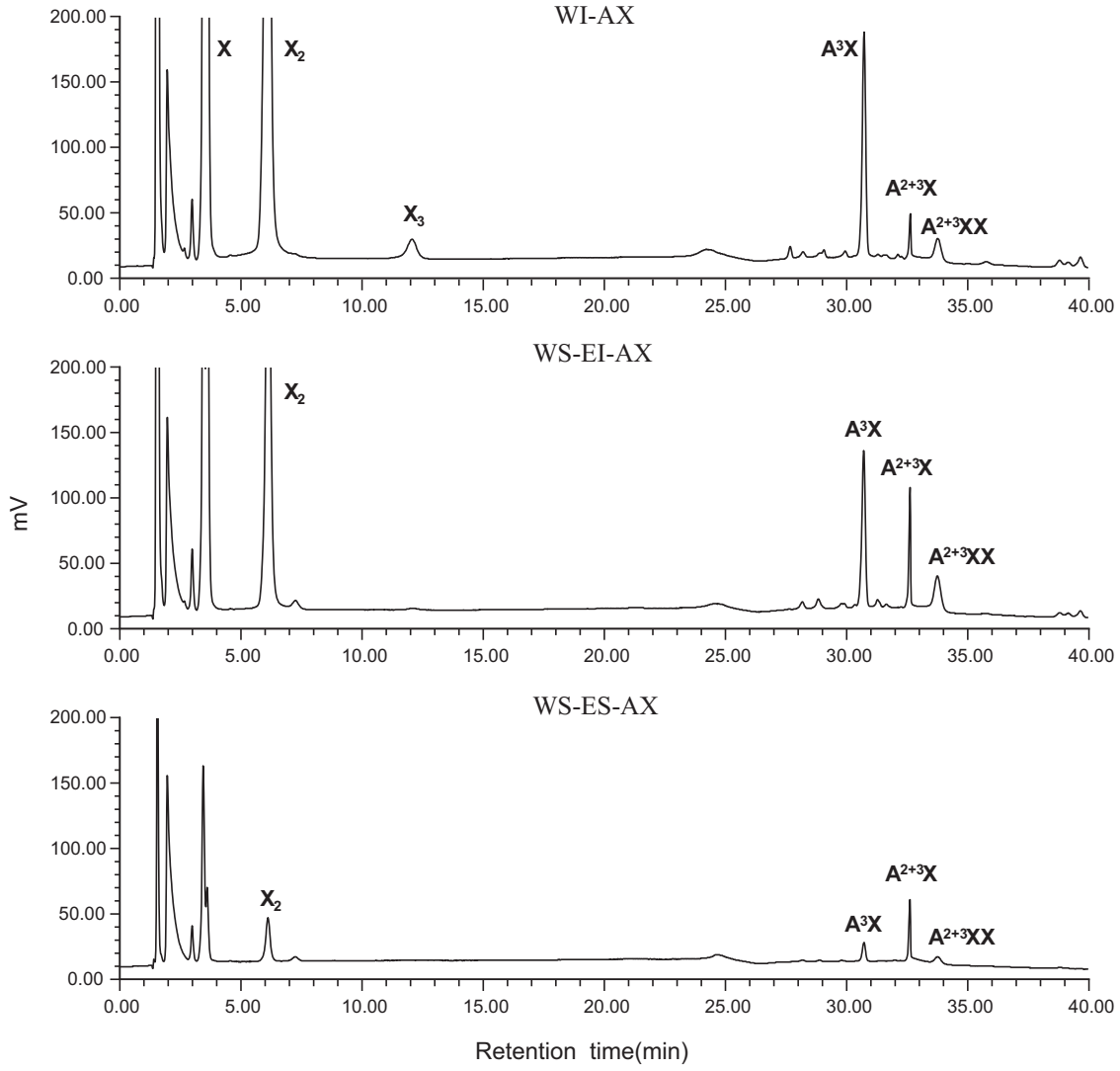

Fig. 2. HPAED-PAD chromatograms of the three AX endoxylanase hydrolysates.

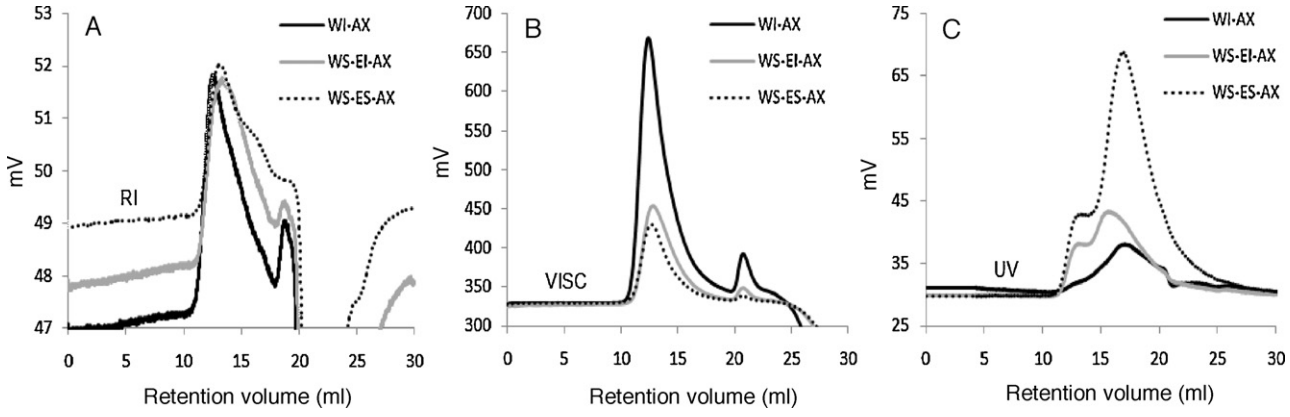

Fig. 3. HPSEC chromatograms of three AX fractions (A: RI signals; B: viscosity signals; C: UV signals).

Table 2
HPSEC analysis of AX.

Sample	M_w (g/mol)	$[\eta]$ (mL/g)	R_h (nm)	L_p (nm)	Recovery (%)
WI-AX	166 000	240	18	2.4	67
WS–EI-AX	152 000	122	14	2.1	64
WS–ES-AX	218 000	116	15	3.0	97

M_w, weight average molar mass; $[\eta]$, intrinsic viscosity; R_h, hydrodynamic radius; L_p, persistence length; R_h has been determined with LS/viscometry method.

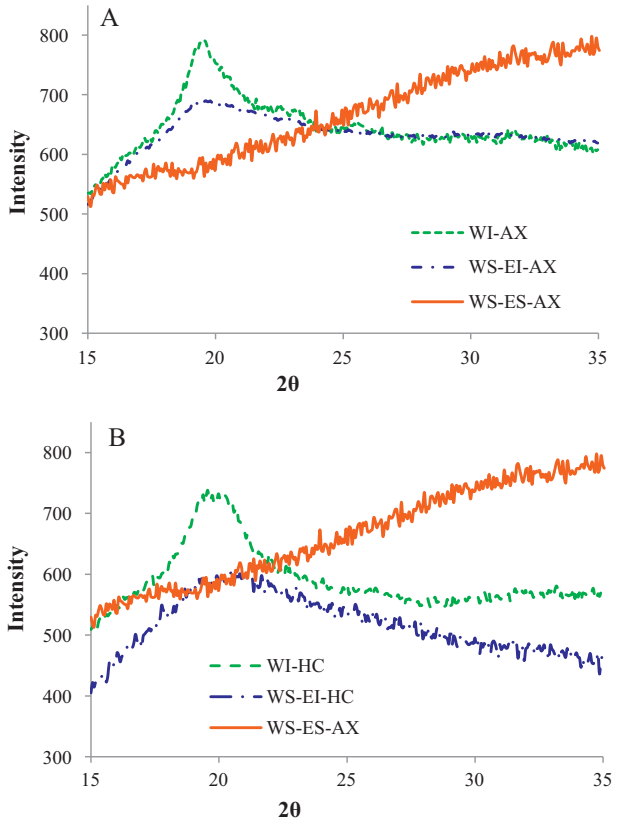

Fig. 4. X-ray diffractograms of films. (A) WI-AX; WS–EI-AX and WS–ES-AX. (B) WI-HC; WS–EI-HC and WS–ES-AX.

been discovered with increasing arabinose-to-xylose ratios in the case of water-soluble, deesterified wheat arabinoxylans (Dervilly, Saulnier, Roger, & Thibault, 2000). The persistence length values (L_p), which describe the rigidity of a polymer, were determined for each AX sample in order to compare their chain stiffness. The L_p value of WS–ES-AX fraction was above the value expected for AX in a good solvent (1.8–2.3 nm) (Pitkanen et al., 2009). High L_p values for β-glucan samples containing aggregates were presented in a recent publication (Li, Cui, Wang, & Yada, 2011). Thus, high L_p values of WS–ES-AX might reflect the presence of aggregates in this fraction.

3.4. Film properties of HC and AX

Films were made both from the HC and AX fractions using the water casting method. As WI-HC and WI-AX fractions were not soluble in water at 60 °C (see the fractionation process), 1 h at 95 °C under mixing was necessary to cast all films with the same methodology. Films from both HC and AX fractions formed homogeneous suspensions which, upon drying, led to qualitatively similar homogeneous and transparent films. The films from WI-AX and WI-HC shrunk greatly during formation, and typical thicknesses were around 50 μm for the WI film and 35 μm for the WS-EI and WS–ES-AX films. The WS–ES-AX film was light yellow, whereas the others almost colorless. This coloration was probably due to the higher lignin content of WS–ES-AX (Table 1).

3.4.1. X-ray analysis

Fig. 4 shows the X-ray diffractograms of the films from various fractions in order to qualitatively study their respective crystalline morphology before and after β-glucan removal. The WS–ES-AX films were obviously amorphous without any crystallinity peak (Fig. 4). The WI-HC and WS–EI-HC films (Fig. 4B) and the corresponding WI-AX and WS–EI-AX (Fig. 4A) have clear diffraction peaks between 17 and 23° (in 2θ). The WI-AX fraction had higher peak intensity, indicating a higher level of organization compared to the WS–EI-AX fraction (Fig. 4A).

The substitution pattern of AX influences the film morphology as substitutions can act as structural defects preventing macromolecule crystallization (Sternemalm, Höije, & Gatenholm, 2008) Consequently, unsubstituted regions along the xylan chains promote crystallization (Dervilly-Pinel, Tran, & Saulnier, 2004). In our study, the crystallinity peak (presence and intensity) was well correlated to the Ara/Xyl ratio as well as the qualitative observation of

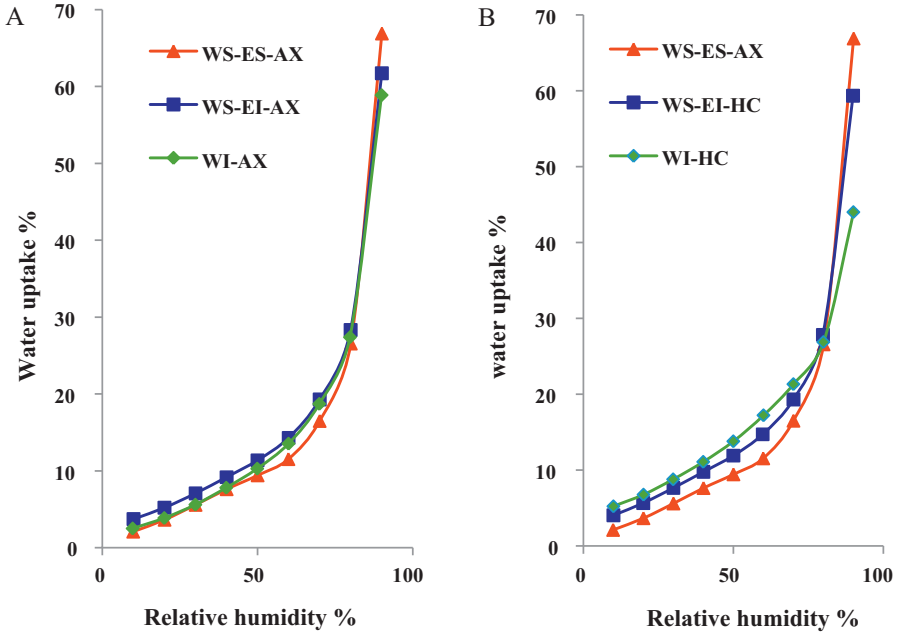

Fig. 5. Water sorption isotherms of arabinoxylans AX (A) and hemicelluloses HC (B) fractions.

Table 3
The beta transitions (sub-Tg) of HC and AX fractions.

		WI-HC	WS–EI-HC	WI-AX	WS–EI-AX	WS–ES-AX
Beta transition (sub-Tg, °C)[a]	54% RH	−56	−47	−19	−38	−64
	85% RH	−61	−49	−38	−53	−67

[a] Sub-Tg measured at 100 000 Hz.

film shrinkage during drying (WI-AX films: Ara/Xyl = 0.23) because of reorganization of this weakly substituted xylan fraction.

Fig. 4 also compares the X-ray results for the films before and after lichenase treatment. After treatment, the peaks were sharper, especially for the WI-AX fractions. It seems that the degree of order is higher for the purified xylans. In case of the HC fractions, the interactions in such polymer blends (β-glucan/AX) are strong enough not to be fractionated during the extraction process and to disturb the level of macromolecule organization.

3.4.2. Water sorption properties

The water sorption isotherms of the films from the AX fractions are presented in Fig. 5A. The relative humidity (RH) scale can be divided into two areas: below 80% where the water molecules are bound by the water AX sorption sites and over 80% where a noticeable increase of water sorption occurs. Below 80% RH, the water content differences were not very large between the samples. Moreover, the curves were not homothetic. This property indicates that the sorption sites on AX chains are not equivalently distributed or available along the macromolecules for the water molecules. This behavior has already been reported by Sternemalm et al. (2008). The difference is not very large and the authors explained that this behavior might be due to interactions between water and hydroxyl groups of unsubstituted units which are not involved in crystalline regions. Over 80% RH, the water uptake increased for all the samples due to film swelling by water, and the differences between the samples were well correlated with their degree of substitution, the WS–ES-AX films having the highest water content whereas the WI-AX showed the lowest one. Water attempts to enter the macromolecular network as in the water sorption process at high RH, but the network achieved by crystallization for the low branched samples prevents the films from swelling by water molecules.

Previous studies (Höije et al., 2008; Sternemalm et al., 2008) have reported the same trend with AX hydration: at high relative humidity, the highly substituted samples showed a higher water uptake than the samples that were enzymatically debranched with an α-arabinosidase treatment. In comparison with our results, Höije et al. (2008) found that the water content of their film was around 41% at 98% RH for AX with an Ara/Xyl ratio of 0.20 against 58% at 90% RH for our WI-AX with an Ara/Xyl ratio of 0.23. This variation could be due to measurement methodology or to a difference in the AX structure (i.e. different substitution patterns between enzymatically treated samples (Höije et al., 2008) and native samples (this study).

The elimination of β-glucans significantly modified the water sorption of WI-HC, as compared to the WS–ES-AX sample which had not been purified by lichenase (Fig. 5B). In fact, for WI-AX, the water content decreased at low RH and increased significantly at high RH. The higher water sorption in the case of purified AX could be due to the absence of β-glucans which, when present, could modify the conformation and the morphology of AX. However, it cannot be excluded that the protein addition during the lichenase/β-glucosidase treatment could also be responsible for the differences in water sorption observed after the enzymatic removal of β-glucans. Meanwhile, at 90% RH, water sorption increases with a higher A/X ratio in the presence or absence of β-glucans.

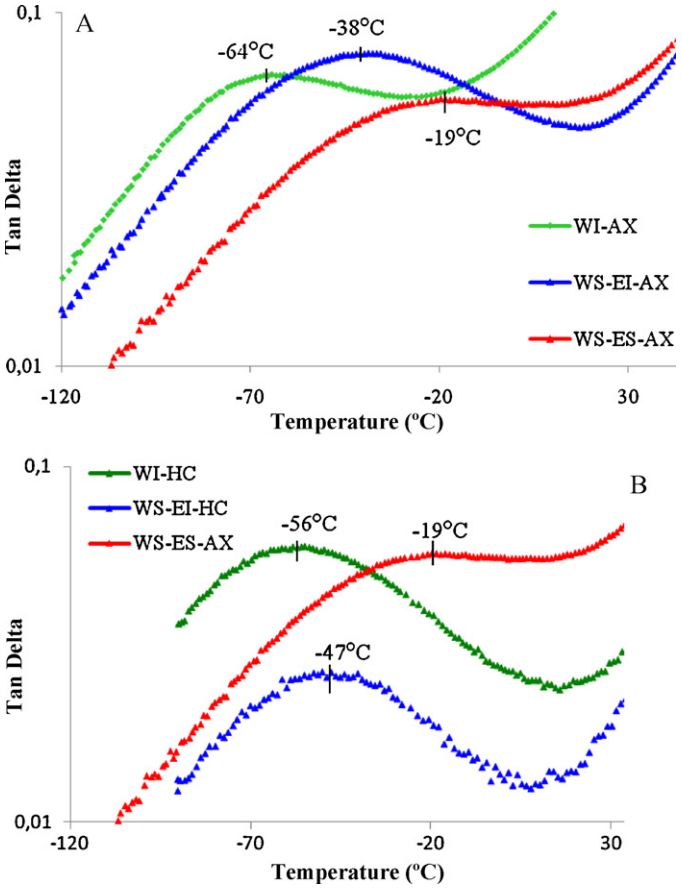

Fig. 6. Dielectric loss tangent of the damping peak *versus* temperature. (A) WI-AX, WS–EI-AX and WS–ES-AX fractions previously hydrated at 54% RH. (B) WI-HC, WS–EI-HC and WS–ES-AX fractions previously hydrated at 54% RH (frequency = 100 000 Hz).

3.4.3. Viscoelastic properties

The viscoelastic properties of the polymer films from the HC and AX fractions were analyzed in order to get information about local macromolecular mobility (beta transitions).

The films were analyzed by dielectric analyzer (DEA) after prehydration (at 54 and 85% RH) and performing a devoted hermetic sensor set-up. Typical thermograms (frequency variation from 1 to 100 000 Hz) presented two relaxations. These could be attributed to a beta transition (sub-Tg) at low temperature, and to the alpha transition linked to the glass transition temperature at higher temperature (data not shown).

In a typical manner, all observed relaxations were shifted to a higher temperature as frequency increased, and to lower temperature when relative humidity increased as expected for water plasticized hydrophilic polymers. The sub-Tg (at the maximum of the tan δ peak) systematically decreased from WS–ES-AX, WS–EI-AX to WI-AX (Fig. 6A) and for the corresponding unpurified fractions (Fig. 6B). Table 3 shows the sub-Tg values obtained for 100 000 Hz at 54 and 85% RH.

This result demonstrated that the sub-Tg was well correlated with the substitution degree as the higher the Ara/Xyl ratio was,

the higher the sub-Tg observed. This higher sub-Tg transition indicated a lower segmental mobility or local AX chain mobility when xylose units are highly substituted by arabinose. This result was systematically obtained whatever the studied relative humidity (54%, 85% RH) or the frequency, even if the signals were obviously easier to monitor at higher water content and frequency, being located between suitable temperature limits.

The same correlation was observed between the sub-Tg and the substitution degree for the three HC fractions before lichenase treatment (Fig. 6B). In these cases the sub-Tg was not systematically shifted in the same way. For example, the sub-Tg of WI-HC was higher than after lichenase purification whereas WS–EI-HC had a lower sub-Tg than WS–EI-AX.

As indicated by the sub-Tg decrease with a lower Ara/Xyl ratio, the local chain motion decreased in the amorphous parts for highly substituted xylans. This loss of mobility could then be related to intermolecular hydrogen bonds which seemed to occur because of the presence of arabinose inside the amorphous part, locally stiffening the AX chain.

4. Conclusion

Different populations of AX were isolated from wheat bran according to a laboratory scale alkali extraction process. After alkali isolation and fractionation according to solubility in water and ethanol, a purification was performed in order to remove β-glucans. Three lots of AX fractions displaying a large range of Ara/Xyl ratios (from 0.2 to 1.3) were obtained. Patterns of α-L-Araf substitutions were proposed according to a fine structural analysis. Molar mass was comprised between 152 000 and 218 000 g/mol.

Films were then made from these characterized fractions in order to study the impact of AX composition and structure on their physico-chemical properties. The main results indicated that the crystalline morphology, the beta transitions as well as the water sorption properties of AX films are well correlated to the substitution degree by arabinose groups. When the substitution degree is low, AX are less soluble in water and ethanol, less hydrophilic at high relative humidity, crystalline morphology appears, and more surprisingly, the local macromolecular mobility increases.

In conclusion, hemicellulose based materials showed physico-chemical properties strongly linked to the native Ara/Xyl ratios controlled by suitable fractionation process conditions.

Acknowledgments

The authors thank Nathalie Aubry, Miguel Pernes, David Crônier, and Olivier Delfosse for technical help and Päivi Tuomainen for the interpretation of HPSEC results. French National Institute of Agronomy (INRA) and the Région Champagne-Ardenne (France) are gratefully acknowledged for their financial support through the Woodwisdom-net Biopack program. The authors also thank Karen Plé for her English proofreading.

COST 928 is acknowledged for financial support of the visit to perform HPAEC-PAD and HPSEC analysis at the University of Helsinki.

References

Andrewartha, K. A., Phillips, D. R., & Stone, B. A. (1979). Solution properties of wheat-flour arabinoxylans and enzymically modified arabinoxylans. *Carbohydrate Research*, *77*, 191–204.

Bataillon, M., Mathaly, P., Nunes Cardinali, A. P., & Duchiron, F. (1998). Extraction and purification of arabinoxylan from destarched wheat bran in a pilot scale. *Industrial Crops and Products*, *8*, 37–43.

Beaugrand, J., Crônier, D., Debeire, P., & Chabbert, B. (2004). Arabinoxylan and hydroxycinnamate content of wheat bran in relation to endoxylanase susceptibility. *Journal of Cereal Science*, *40*, 223–230.

Benamrouche, S., Crônier, D., Debeire, P., & Chabbert, B. (2002). A chemical and histological study on the effect of (1 → 4)-β-endo-xylanase treatment on wheat bran. *Journal of Cereal Science*, *36*, 253–260.

Bergmans, M. E. F., Beldman, G., Gruppen, H., & Voragen, A. G. J. (1996). Optimisation of the selective extraction of (glucurono) arabinoxylans from wheat bran: Use of barium and calcium hydroxide solution at elevated temperatures. *Journal of Cereal Science*, *23*, 235–245.

Bohdanecky, M. (1983). New method for estimating the parameters of the wormlike chain model from the intrinsic viscosity of stiff-chain polymers. *Macromolecules*, *16*, 1483–1492.

Brillouet, J. M., Joseleau, J. P., Utille, J. P., & Lelievre, D. (1982). Isolation, purification and characterization of a complex heteroxylan from industrial wheat bran. *Journal of Agricultural and Food Chemistry*, *30*, 488–495.

Dervilly, G., Saulnier, L., Roger, P., & Thibault, J. F. (2000). Isolation of homogeneous fractions from wheat water-soluble arabinoxylans. Influence of the structure on their macromolecular characteristics. *Journal of Agricultural and Food Chemistry*, *48*, 270–278.

Dervilly-Pinel, G., Tran, V., & Saulnier, L. (2004). Investigation of the distribution of arabinose residues on the xylan backbone of water-soluble arabinoxylans from wheat flour. *Carbohydrate Polymers*, *55*, 171–177.

Dole, P., Joly, C., Espuche, E., Alric, I., & Gontard, N. (2004). Gas transport properties of starch based films. *Carbohydrate Polymers*, *58*, 335–343.

Ebringerová, A. (2005). Structural diversity and application potential of hemicelluloses. *Macromolecular Symposia*, *232*, 1–12.

Ebringerova, A., & Heinze, T. (2000). Xylan and xylan derivatives – Biopolymers with valuable properties. 1. Naturally occurring xylans structures, procedures and properties. *Macromolecular Rapid Communications*, *21*, 542–556.

Fishman, M. L., Doner, L. W., Chau, H. K., & Hoagland, P. D. (2000). Characterization of hemicellulose B from corn fiber by high-performance size exclusion chromatography with on-line molar mass and viscometric detection. *International Journal of Polymer Analysis and Characterization*, *5*, 359–379.

Goring, D. A. I., & Timell, T. E. (1960). Molecular properties of six 4-O-methylglucuronoxylans. *The Journal of Physical Chemistry*, *64*, 1426–1430.

Grondahl, M., Eriksson, L., & Gatenholm, P. (2004). Material properties of plasticized hardwood xylans for potential application as oxygen barrier films. *Biomacromolecules*, *5*, 1528–1535.

Hansen, N. M. L., & Plackett, D. (2008). Sustainable films and coatings from hemicelluloses: A review. *Biomacromolecules*, *9*, 1493–1505.

Hartman, J., Albertsson, A. C., Lindblad, M. S., & Sjoberg, J. (2006). Oxygen barrier materials from renewable source: Materials properties of softwood hemicellulose-based films. *Journal of Applied Polymer Science*, *100*, 2985–2991.

Henry, R. J., Martin, D. J., & Blakeney, A. B. (1987). Reduction of the [alpha]-amylase content of sprouted wheat by pearling and milling. *Journal of Cereal Science*, *5*, 155–166.

Höije, A., Gröndahl, M., Tømmeraas, K., & Gatenholm, P. (2005). Isolation and characterization of physicochemical and material properties of arabinoxylans from barley husks. *Carbohydrate Polymers*, *61*, 266–275.

Höije, A., Sternemalm, E., Heikkinen, S., Tenkanen, M., & Gatenholm, P. (2008). Material properties of films from enzymatically tailored arabinoxylans. *Biomacromolecules*, *9*, 2042–2047.

Hong, S.-I., & Krochta, J. M. (2006). Oxygen barrier performance of whey–protein-coated plastic films as affected by temperature, relative humidity, base film and protein type. *Journal of Food Engineering*, *77*, 739–745.

Izydorczyk, M. S., & Biliaderis, C. G. (2000). Structural and functional aspects of cereal arabinoxylans and β-glucans. *Developments in Food Science*, *41*, 361–384.

Li, W., Cui, S. W., Wang, Q., & Yada, R. Y. (2011). Studies of aggregation behaviours of cereal β-glucans in dilute aqueous solutions by light scattering: Part I. Structure effects. *Food Hydrocolloids*, *25*, 189–195.

Monties, B. (1984). Dosage de la lignine insoluble en milieu acide: Influence du prétraitement par hydrolyse acide sur la lignine Klason de bois et de paille. *Agronomie*, *4*, 387–392.

Nishimura, T., Ishihara, M., Ishii, T., & Kato, A. (1998). Structure of neutral branched xylooligosaccharides produced by xylanase from in situ reduced hardwood xylan. *Carbohydrate Research*, *308*, 117–122.

Pastell, H. (2010). *Thesis, University of Helsinki*.

Pastell, H., Tuomainen, P., Virkki, L., & Tenkanen, M. (2008). Step-wise enzymaticpreparation and structural characterization of singly and doubly substituted arabinoxylo-oligosaccharides with non-reducing end terminal branches. *Carbohydrate Research*, *343*, 3049–3057.

Pastell, H., Virkki, L., Harju, E., Tuomainen, P., & Tenkanen, M. (2009). Presence of 1 → 3-linked 2-O-β-D-xylopyranosyl-α-L-arabinofuranosyl side chains in cereal arabinoxylans. *Carbohydrate Research*, *344*, 2480–2488.

Pitkanen, L., Virkki, L., Tenkanen, M., & Tuomainen, P. (2009). Comprehensive multidetector HPSEC study on solution properties of cereal arabinoxylans in aqueous and DMSO solutions. *Biomacromolecules*, *10*, 1962–1969.

Ring, S. G., & Selvendran, R. R. (1980). Isolation and analysis of cell wall material from beeswing wheat bran (*Triticum aestivum*). *Phytochemistry*, *19*, 1723–1730.

Sternemalm, E., Höije, A., & Gatenholm, P. (2008). Effect of arabinose substitution on the material properties of arabinoxylan films. *Carbohydrate Research*, *343*, 753–757.

Vertucci, C. W., & Roos, E. E. (1993). Theoretical basis of protocols for seed storage. II. The influence of temperature on optimal moisture levels. *Seed Science Research*, *3*, 201–213.

Zinbo, M., & Timell, T. E. (1965). The degree of branching of hardwood xylans. *Svensk Papperstid*, *68*, 647–662.